Journal of Magnetism and Magnetic Materials 564 (2022) 170052

Contents lists available at ScienceDirect

Journal of Magnetism and Magnetic Materials

journal homepage: www.elsevier.com/locate/jmmm

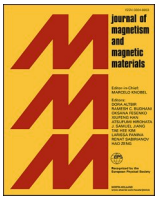

Effects of atomic layer etching on magnetic properties of CoFeB films: Reduction of Gilbert damping

Mahsa Konh [a,1], Yang Wang [b,1], Marissa Pina [a,1], Andrew V. Teplyakov [a], John Q. Xiao [b,*]

[a] Department of Chemistry and Biochemistry, University of Delaware, Newark, DE 19716, USA
[b] Department of Physics and Astronomy, University of Delaware, Newark, DE 19716, USA

ARTICLE INFO

Keywords:
CoFeB
Atomic layer etching
Ferromagnetic resonance
Gilbert damping

ABSTRACT

Atomic layer etching (ALE) is an emerging technology to etch thin films with atomic level precision for microelectronics industry applications. This approach has been previously demonstrated to work on a number of materials; however, in most cases, only electronic properties of these materials following ALE are investigated. Since ALE of complex magnetic materials is extremely important for use in magnetic tunnel junctins (MTJs), it is imperative to understand how this etching approach affects the magnetic properties of the corresponding films. In this work, we studied the surface morphology, elemental composition, and most importantly, the magnetic properties of the technologically relevant magnetic alloy CoFeB before and after ALE treatment, and compared with the traditional ion milling etching technique. Through ferromagnetic resonance measurements, we find while the change in the saturation magnetization from ALE is small, the Gilbert damping of CoFeB is reduced by 11–35%, possibly due to the suppressed two-magnon scattering processes on the sample surface. Our results show that ALE can be used to etch CoFeB nondestructively and may even improve its magnetization dynamics properties.

1. Introduction

Spintronics aims at controlling magnetic elements through electrical means for storage or computing purposes [1–4]. Although in recent years, novel magnetic materials like ferrimagnetic iron garnet [5–7], antiferromagnets [8,9], and van der Waals magnets [10–12] have been intensively explored for different merits, traditional ferromagnetic transition metals (Co, Fe, Ni) and their alloys still remain the most applicable materials because of ease of deposition, fabrication, and mass-production, not to mention their high Curie temperatures and chemical stability which all have been taken for granted. Taking CoFeB alloy as an example, magnetic tunnel junctions (MTJs) with robust perpendicular magnetic anisotropy [13] and electrical switchability [14] have been successfully achieved in CoFeB/MgO heterostructures deposited by industrial friendly magnetron-sputtering method on cost-friendly silicon wafers.

In order to make compact devices with large number of basic magnetic elements like MTJs, the heterostructures need to be fabricated into nanometer-scale dimensions which calls for processing techniques with atomic level precision. In the past three decades, atomic layer etching (ALE) [15–17] has been demonstrated to be able to etch semiconductors [18,19], oxides [20,21], and metals [22–26] layer by layer, thanks to its self-limiting nature. While previous ALE studies typically focused on the etching mechanisms, change in surface roughness and chemical compositions, for magnetic materials, investigating the effects on magnetic properties is crucial for applying the ALE technique to potential spintronic devices.

In this work, we studied the surface morphology, elemental composition and magnetic properties of CoFeB films before and after ALE treatment, and compared with the analogous samples prepared by ion milling method. The change in saturation magnetization is within 2%. The Gilbert damping constant, measured by the ferromagnetic resonance (FMR) method, is found to be reduced significantly by 11–35% after the ALE procedures, while it was increased by 11% in the ion-milled sample. From the atomic force microscopy (AFM) and x-ray photoelectron spectroscopy (XPS) results we hypothesize that the chemical adsorption and desorption procedures in ALE cycles may help reduce the number of scattering centers on the CoFeB surface, so the two-magnon scattering (TMS) contribution is suppressed, resulting in a lower Gilbert damping constant.

* Corresponding author.
E-mail address: jqx@udel.edu (J.Q. Xiao).
[1] These authors contributed equally.

https://doi.org/10.1016/j.jmmm.2022.170052
Received 24 August 2022; Received in revised form 27 September 2022; Accepted 6 October 2022
Available online 17 October 2022

2. Methods

The CoFeB films used in this study were sputter-deposited on thermally oxidized silicon wafers at room temperature in a home-built system with base pressure of 3×10^{-7} Torr. The commercially purchased target (ACI Alloys) has a nominal atomic ratio Co:Fe:B = 20:60:20. The DC power was set to 18 W and the Ar pressure was 3 mTorr during the deposition. Sample A was deposited in an off-axis sweeping mode to achieve a wedge profile with thicknesses 21.1 nm and 40.2 nm on the two ends. Areas with thicknesses of 40.2 nm and 37.8 nm were selected from Sample A for ALE and ion-milling etching, respectively. Sample B with a uniform 35 nm thickness was deposited at a different time with a higher base pressure. The thicknesses of the films were measured by the x-ray reflectivity method.

Atomic force microscopy (AFM) was used to determine the roughness of the alloy surface. The RMS roughness of each image was determined using Gwyddion software. The surface composition of the alloy was analyzed *ex-situ* on a K-alpha + XPS system using an Al K-alpha x-ray source ($h\nu = 1486.6$ eV) at a 35.3° takeoff angle with respect to the analyzer. For quantitative analysis, peaks were fitted using a Shirley background and a Gaussian/Lorentzian lineshape and calibrated by the C 1s peak at 284.6 eV observed in all the experiments for adventitious carbon.

As summarized in Fig. 1a, atomic layer etching of the CoFeB alloy was performed in an ultra-high vacuum (UHV, base pressure 10^{-9} Torr) chamber. The sample was attached to a button heater with a tantalum collar. It was annealed at 440 K for 40 min and then chlorinated using a home-built solid-state electrochemical cell based on silver chloride and cadmium chloride. Auger electron spectroscopy was used to confirm the presence of chlorine on the surface and to determine the dosing time needed to form a saturated layer similarly to the previously reported procedure [26]. After surface modification by chlorine, 300 Langmuir of acetylacetone (acacH) was dosed into the chamber. This exposure was chosen based on the previously reported work [26] and determined to be sufficient to remove surface chlorine-containing species based on the post-exposure XPS investigations. A Hiden Analytical mass spectrometer was used to test the purity of acacH *in-situ*. Sample A went through 30 full cycles of chlorination and acacH exposure before being removed from the chamber. Sample B was dosed with chlorine one time to determine the effects of surface chlorination on the magnetic properties of the alloy.

The ion mill etching was carried out in a Intlvac Nanoquest I ion beam etching system with off-axis Ar^+ ion beam with 400 eV energy. The sample was mounted on a rotating water-cooled stage. As schematically shown in Fig. 1b, compared with ALE, ion milling is purely a physical etching process which deposits a large amount of energy to the film surface. The magnetic properties of the CoFeB films were investigated through broadband FMR measurements [27] under an in-plane (IP) field setup. The samples were spin-coated with AZ1512 photoresist to avoid shunting of the coplanar waveguide (CPW) line. Both the microwave generation and transmission detection were carried out using an Agilent vector network analyzer.

3. Results and discussions

3.1. Surface morphology and composition characterizations

Fig. 2 shows the AFM results of three as-deposited, ALE, and ion-milled CoFeB films, all taken from the same Sample A. While ion milling yields a slightly higher surface roughness (0.50 nm as compared to 0.34 nm), the film after ALE treatment maintains the surface roughness R_a, consistent with previous reports [24,26]. This observation is not surprising and is fully consistent with previously reported smoothing of the material surface following ALE, which tends to remove adatoms much more easily than the atoms within the terrace sites [24,25]. Fig. 3 displays the XPS peaks for Co, Fe, and B in these three samples. The extracted composition ratios are listed in Table 1. Following 30 cycles of ALE, the Co:Fe:B ratio remains nearly the same as in the original, as deposited sample, while in the ion-milled sample, boron content is significantly reduced. This maybe due to the preferential removal of the light elements during the high-energy Ar^+ ion bombardment process [28]. Therefore, it is not surprising that the surface roughness is also increased in the ion-milled CoFeB film surface. It should also be noted that according to the XPS investigations, the oxidation of the magnetic metals, Co and Fe, does not seem to depend on the sample preparation method. At the same time, the B 1s XPS spectra in Fig. 3 appear to suggest that in ion-milled samples, boron oxidation is less significant than in ALE-treated samples. However, closer comparison of the spectra and the results summarized in Table 1 suggests that it is not that the degree of boron oxidation within surface layers (which is what is measured by XPS) is lower in ion-milled samples, but rather simply the amount of boron in these surface regions, that is different in ion-milled samples compared to ALE-treated ones.

3.2. FMR measurements

The representative FMR absorption intensities as a function of magnetic field H results at 12 GHz are plotted in Fig. 4(a). The inset shows a schematic of the FMR setup, where the sample was placed on a coplanar wave guide (CPW) and an external magnetic field was swept along the signal line direction. The data are fitted with Lorentzian curves to extract the resonance field H_{res} and the full width at half maximum ΔH. As shown in Fig. 4(b), the extracted H_{res} at different frequencies were fitted to the Kittel equation [27].

$$f = \frac{\gamma}{2\pi}\sqrt{(H_{res} + H_a)(H_{res} + 4\pi M_s + H_a)} \tag{1}$$

to obtain the saturation magnetization $4\pi M_s$. H_a is the surface anisotropy field of the thin film. The gyromagnetic ratio γ was fixed at 28 GHz/T. Linewidth ΔH as a function of frequency was fitted with the equation [29].

$$\Delta H = \Delta H_0 + \frac{4\pi\alpha_{eff}}{\gamma} f \tag{2}$$

where ΔH_0 is the inhomogeneous broadening and α_{eff} is the effective Gilbert damping constant, which includes both intrinsic and extrinsic

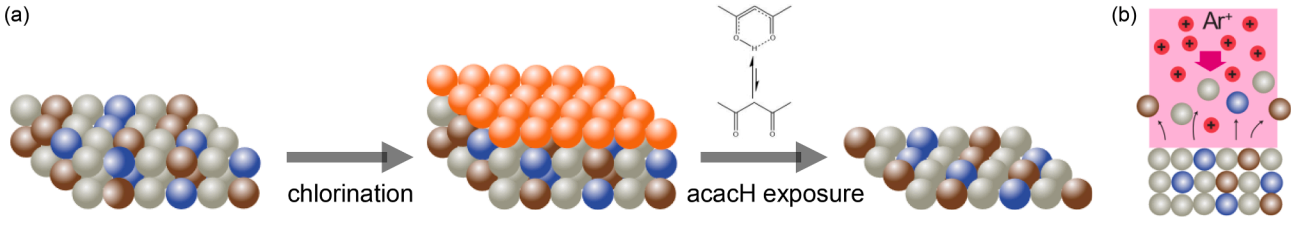

Fig. 1. (a) Atomic layer etching of CoFeB alloy. The first ALE half-cycle consists of chlorination at 440 K for 40 min. Chlorination of the sample results in a modified (oxidized) surface layer. To complete the second half-cycle, 300 L of acetylacetone is dosed at 440 K. (b) Ion beam etching of CoFeB. High energy Ar ions are accelerated to bombard the sample surface and the top most atoms are removed.

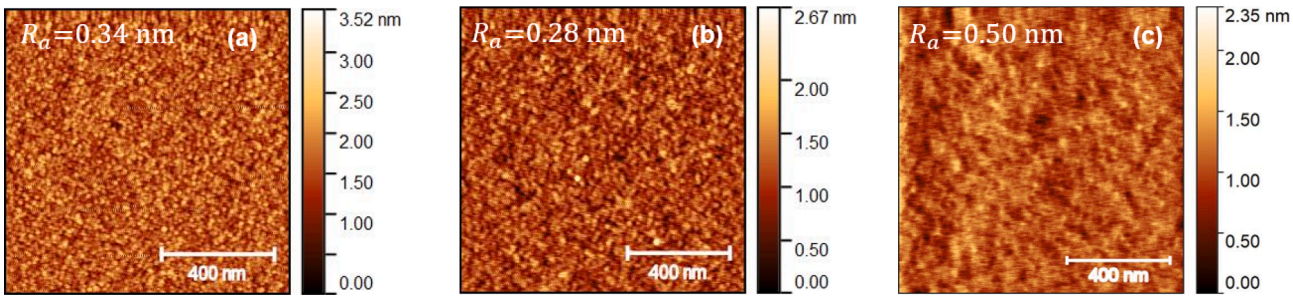

Fig. 2. Atomic force microscope images of (a) As-deposited, (b) ALE, and (c) Ion-milled CoFeB samples. The measured area is 1 × 1μm.

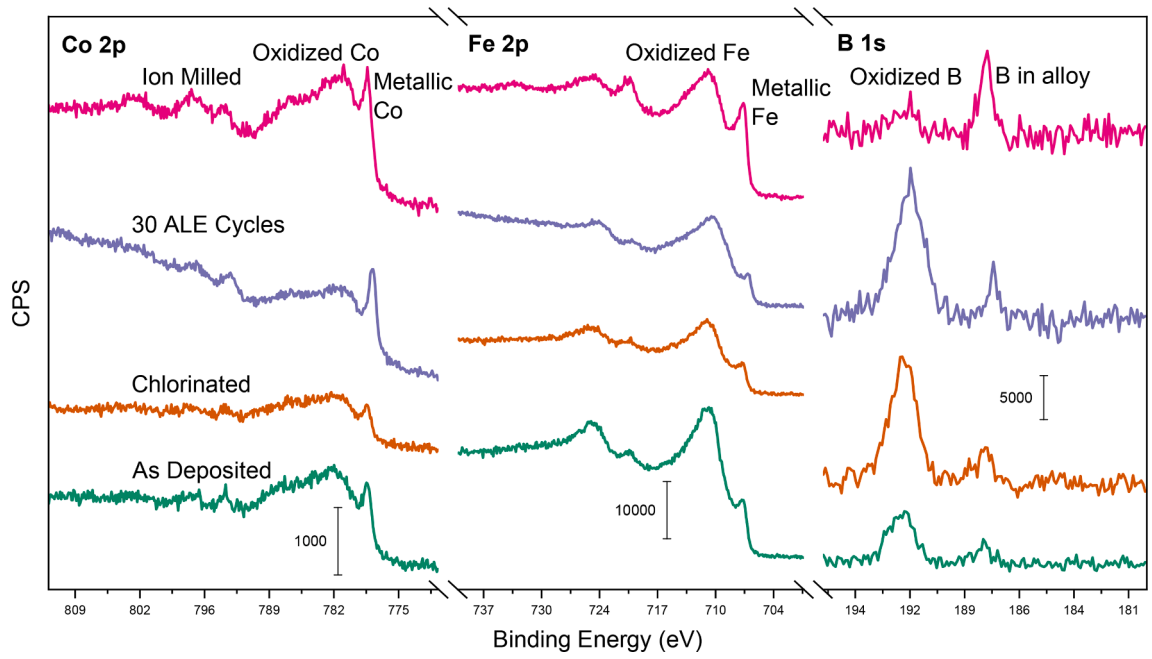

Fig. 3. X-ray photoelectron spectroscopy results of the As-Deposited, Chlorinated, 30 ALE Cycles, and Ion-milled CoFeB films.

Table 1
Thickness, surface roughness R_a, chemical composition, saturation magnetization $4\pi M_s$, and effective Gilbert damping α_{eff} of the As deposited, ALE, and Ion-milled CoFeB films taken from the same original Sample A.

	As Dep.	ALE	Ion mill
Thickness (nm)	34.6	34.1	33.0
R_a(nm)	0.34	0.28	0.50
Co:Fe:B	17:45:37	15:42:43	23:62:15
$4\pi M_s$ (kOe)	18.44 ± 0.02	18.15 ± 0.02	18.48 ± 0.02
α_{eff}(× 10^{-3})	4.6 ± 0.1	4.1 ± 0.1	5.1 ± 0.1

contributions [30,31]. As shown in Table 1, after 30 cycles of ALE, the saturation magnetization $4\pi M_s$ shows a very slight decrease. However, in another set of ALE + FMR experiments on Sample B (Table 2), we find a very slight increase in $4\pi M_s$, so currently we can only conclude that the change on $4\pi M_s$ brought by the ALE process is within 2%. As to the effective Gilbert damping α_{eff}, surprisingly, we find a large, 11–35% decrease of it in all our experiments, including 30 cycles ALE, single chlorination, and 1 cycle chlorination plus acacH exposure.

Gilbert damping is a phenomenological parameter describing the relaxation rate of a magnetic material in magnetization dynamics. It can be parsed into intrinsic and extrinsic contributions [32,33]. The intrinsic damping is governed by intra- or inter-band transitions in the electron-phonon scattering processes [32], while the extrinsic damping for a single magnetic layer includes two-magnon scattering, eddy-current, and radiative contributions. We notice that besides the chemical reactions, during the ALE process the sample was annealed at 440 K. To check whether the reduction in Gilbert damping is from annealing, we annealed two CoFeB films cut from the same original Sample A at 440 K for 6 h in a high vacuum chamber. The FMR measurements on them yield damping constants of 4.53 ± 0.06 × 10^{-3} and 4.84 ± 0.06 × 10^{-3}, respectively. Therefore, annealing alone cannot account for the reduced Gilbert damping in ALE-treated samples. Since the crystalline- and band-structure of the CoFeB films are not affected by surface etching methods, the intrinsic contribution to the Gilbert damping should remain the same. Because the three samples in Table 1 have similar dimensions and bulk properties, the extrinsic eddy-current and radiative damping contributions should not vary much among them. This leads us to consider the suppression/enhancement of TMS processes as the reason for the decrease/increase of Gilbert damping in the ALE/ion-milled samples. It is known that the scattering centers on the surface of a magnetic film plays a dominant role in TMS [33]. The AFM and XPS measurements already revealed that ion milling can introduce more structural or chemical inhomogeneities to the CoFeB film surface, which is likely to enhance the extrinsic damping mechanism through TMS. This is consistent with previous reports [34,35] where magnetic properties of thin films were found to be degraded during ion milling. Oppositely, we speculate that during the chemical adsorption and desorption ALE procedures, the surface defect density of the CoFeB films was reduced, so the TMS is suppressed, resulting in a smaller damping constant as

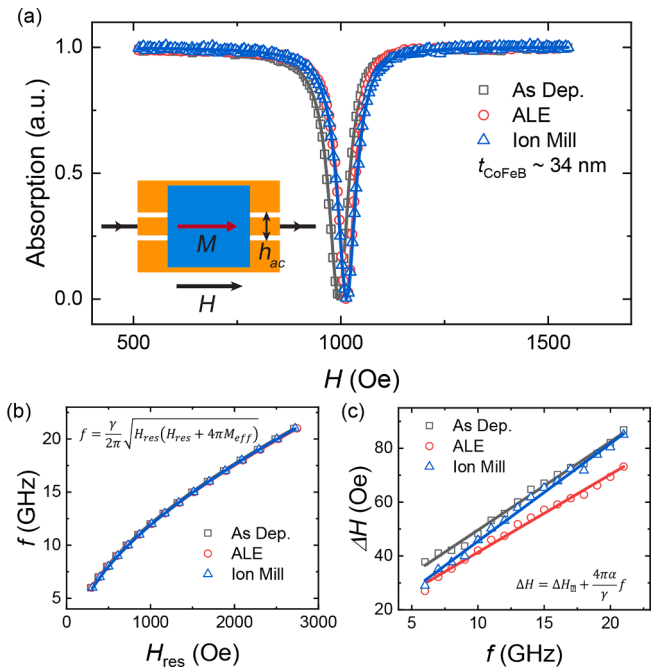

Fig. 4. (a) Ferromagnetic resonance absorption of the As deposited, ALE, and Ion-milled CoFeB films, all cut from Sample A. The inset illustrates the measurement setup. (b) Microwave frequency as a function of the resonance field for the three samples. (c) Linewidth as a function of frequency. In (a)-(c) solid lines are fittings.

Table 2
Effective saturation magnetization $4\pi M_s$ and effective Gilbert damping α_{eff} of Sample B before and after Chlorine, or Chlorine + acacH treatment.

	As Dep.	Chlorine	Chlorine + acacH
$4\pi M_s$ (kOe)	18.53 ± 0.01	18.67 ± 0.02	18.70 ± 0.02
$\alpha_{eff}(\times 10^{-3})$	8.2 ± 0.4	6.8 ± 0.3	5.3 ± 0.3

compared to the original film. As reported in previous studies [30,31,36], the extrinsic TMS disappears when the magnetization is pulled to be perpendicular to the film by the external magnetic field. Due to the magnetic field limit of our setup, we were not able to extract the TMS contribution by performing FMR measurements under perpendicular field. However, this remains a good method to test our hypothesis.

4. Conclusion

In spintronic and magnonic devices, and emerging quantum information processing applications, it is crucially important to reduce the Gilbert damping of the magnetic materials, so the device can operate more efficiently or propagate information over a longer distance. Our comparative study on CoFeB films reveal that compared with conventional ion milling etching method, ALE not only preserves the surface smoothness and chemical composition of the film, but can also help reduce the Gilbert damping constant by dramatic 11–35%. It was already demonstrated that $Co_{25}Fe_{75}$ alloys made by magnetron sputtering can have a damping constant as low as $\sim 1 \times 10^{-3}$ [37], approaching those of ferrimagnetic insulators. Our results suggest that the Gilbert damping of this conventional but highly applicable material can be further reduced by ALE treatment.

CRediT authorship contribution statement

Mahsa Konh: Investigation, Data curation, Writing – review & editing. **Yang Wang:** Investigation, Methodology, Data curation, Writing – original draft. **Marissa Pina:** Investigation, Data curation, Writing – review & editing. **Andrew V. Teplyakov:** Methodology, Data curation, Writing – review & editing, Funding acquisition. **John Q. Xiao:** Conceptualization, Methodology, Writing – review & editing, Funding acquisition.

Declaration of Competing Interest

The authors declare that they have no known competing financial interests or personal relationships that could have appeared to influence the work reported in this paper.

Data availability

Data will be made available on request.

Acknowledgments

This work was supported by the National Science Foundation (CMMI2035354).

References

[1] S.A. Wolf, D.D. Awschalom, R.A. Buhrman, J.M. Daughton, S. von Molnár, M. L. Roukes, A.Y. Chtchelkanova, D.M. Treger, Spintronics: a spin-based electronics vision for the future, Science 294 (5546) (2001) 1488–1495.
[2] I. Žutić, J. Fabian, S. Das Sarma, Spintronics: Fundamentals and applications, Rev. Mod. Phys. 76 (2) (2004) 323–410.
[3] S.D. Bader, S.S.P. Parkin, Spintronics, Annu. Rev. Condens. Matter. Phys. 1 (1) (2010) 71–88.
[4] A. Manchon, I.M. Miron, T. Jungwirth, J. Sinova, J. Zelezny, A. Thiaville, K. Garello, P. Gambardella, Current-induced spin-orbit torques in ferromagnetic and antiferromagnetic systems, Rev. Mod. Phys. 91 (2019), 035004, https://doi.org/10.1103/RevModPhys.91.035004.
[5] H.C. Chang, P. Li, W. Zhang, T. Liu, A. Hoffmann, L.J. Deng, M.Z. Wu, Nanometer-Thick Yttrium Iron Garnet Films With Extremely Low Damping, IEEE Magn. Lett. 5 (2014) 6700104, https://doi.org/10.1109/LMAG.2014.2350958.
[6] T. Liu, H.C. Chang, V. Vlaminck, Y.Y. Sun, M. Kabatek, A. Hoffmann, L.J. Deng, M. Z. Wu, Ferromagnetic resonance of sputtered yttrium iron garnet nanometer films, J. Appl. Phys. 115 (2014) 17A501, https://doi.org/10.1063/1.4852135.
[7] C.O. Avci, A. Quindeau, C.-F. Pai, M. Mann, L. Caretta, A.S. Tang, M.C. Onbasli, C. A. Ross, G.S.D. Beach, Current-induced switching in a magnetic insulator, Nat. Mater. 16 (3) (2017) 309–314.
[8] T. Jungwirth, X. Marti, P. Wadley, J. Wunderlich, Nat. Nanotechnol. 11 (2016) 231, https://doi.org/10.1038/nnano.2016.18.
[9] V. Baltz, A. Manchon, M. Tsoi, T. Moriyama, T. Ono, Y. Tserkovnyak, Rev. Mod. Phys. 90 (2018), 015005, https://doi.org/10.1103/RevModPhys.90.015005.
[10] C. Gong, L. Li, Z. Li, H. Ji, A. Stern, Y. Xia, T. Cao, W. Bao, C. Wang, Y. Wang, Z. Q. Qiu, R.J. Cava, S.G. Louie, J. Xia, X. Zhang, Discovery of intrinsic ferromagnetism in two-dimensional van der Waals crystals, Nature 546 (7657) (2017) 265, https://doi.org/10.1038/nature22060.
[11] B. Huang, G. Clark, E. Navarro-Moratalla, D.R. Klein, R. Cheng, K.L. Seyler, D. Zhong, E. Schmidgall, M.A. McGuire, D.H. Cobden, W. Yao, D.i. Xiao, P. Jarillo-Herrero, X. Xu, Layer-Dependent Ferromagnetism in a van der Waals Crystal down to the Monolayer Limit, Nature (London) 546 (7657) (2017) 270–273.
[12] M. Gibertini, M. Koperski, A. Morpurgo, K. Novoselov, M. Gibertini, M. Koperski, A. Morpurgo, K. Novoselov, Nat. Nanotechnol. 14 (2019) 408, https://doi.org/10.1038/s41565-019-0438-6.
[13] S. Ikeda, K. Miura, H. Yamamoto, K. Mizunuma, H.D. Gan, M. Endo, S. Kanai, J. Hayakawa, F. Matsukura, H. Ohno, A perpendicular-anisotropy CoFeB–MgO magnetic tunnel junction, Nat. Mater. 9 (9) (2010) 721–724.
[14] W.-G. Wang, M. Li, S. Hageman, C.L. Chien, Electric-field-assisted switching in magnetic tunnel junctions, Nat. Mater. 11 (2011) 64, https://doi.org/10.1038/nmat3171.
[15] K.J. Kanarik, T. Lill, E.A. Hudson, S. Sriraman, S. Tan, J. Marks, V. Vahedi, R. A. Gottscho, Overview of atomic layer etching in the semiconductor industry, J. Vac. Sci. Technol. A 33 (2) (2015), 020802, https://doi.org/10.1116/1.4913379.
[16] S.M. George, Y. Lee, Prospects for Thermal atomic layer etching using sequential, self-limiting fluorination and ligand-exchange reactions, ACS Nano 10 (5) (2016) 4889–4894, https://doi.org/10.1021/acsnano.6b02991.
[17] Y. Tsai, Z. Li, S. Hu, Recent Progress of Atomic Layer Technology in Spintronics: Mechanism, Mater. Prosp. Nanomater. 12 (2022) 661, https://doi.org/10.3390/nano12040661.
[18] P.A. Maki, D.J. Ehrlich, Laser bilayer etching of GaAs surfaces, Appl. Phys. Lett. 55 (2) (1989) 91–93.
[19] S.D. Athavale, D.J. Economou, Realization of atomic layer etching of silicon, J. Vac. Sci. Technol. B 14 (1996) 3702, https://doi.org/10.1116/1.588651.

[20] J.W. DuMont, A.E. Marquardt, A.M. Cano, S.M. George, Thermal Atomic Layer Etching of SiO_2 by a "Conversion-Etch" Mechanism Using Sequential Reactions of Trimethylaluminum and Hydrogen Fluoride, ACS Appl. Mater. Interfaces 9 (11) (2017) 10296–10307.
[21] Y. Lee, S.M. George, Atomic Layer Etching of Al_2O_3 Using Sequential, Self-Limiting Thermal Reactions with Sn(acac)2 and HF, ACS Nano 9 (2015) 2061–2070, https://doi.org/10.1021/nn507277f.
[22] J. Zhao, M. Konh, A. Teplyakov, Surface chemistry of thermal dry etching of cobalt thin films using hexafluoroacetylacetone (hfacH), Appl. Surf. Sci. 455 (2018) 438–445, https://doi.org/10.1016/j.apsusc.2018.05.182.
[23] J.W. Park, D.S. Kim, W.O. Lee, J.E. Kim, G.Y. Yeom, Atomic layer etching of chrome using ion beams, Nanotechnology 30 (8) (2019) 085303, https://doi.org/10.1088/1361-6528/aaf521.
[24] M. Konh, C. He, X.i. Lin, X. Guo, V. Pallem, R.L. Opila, A.V. Teplyakov, Z. Wang, B. o. Yuan, Molecular mechanisms of atomic layer etching of cobalt with sequential exposure to molecular chlorine and diketones, J. Vac. Sci. Technol. A 37 (2) (2019) 021004, https://doi.org/10.1116/1.5082187.
[25] M. Konh, A. Janotti, A. Teplyakov, Molecular mechanism of thermal dry etching of iron in a two-step atomic layer etching process: chlorination followed by exposure to acetylacetone, J. Phys. Chem. C 125 (13) (2021) 7142–7154, https://doi.org/10.1021/acs.jpcc.0c10556.
[26] M. Konh, Y. Wang, H. Chen, S. Bhatt, J.Q. Xiao, A.V. Teplyakov, Selectivity in atomically precise etching: Thermal atomic layer etching of a CoFeB alloy and its protection by MgO, Appl. Surf. Sci. 575 (2022), 151751, https://doi.org/10.1016/j.apsusc.2021.151751.
[27] I.S. Maksymov, M. Kostylev, Broadband stripline ferromagnetic resonance spectroscopy of ferromagnetic films, multilayers and nanostructures, Physica E 69 (2015) 253, https://doi.org/10.1016/j.physe.2014.12.027.
[28] S.J. Pearton, U.K. Chakrabarti, A.P. Perley, K.S. Jones, Ion milling damage in InP and GaAs, J. Appl. Phys. 68 (6) (1990) 2760–2768.
[29] J.-M.-L. Beaujour, W. Chen, A.D. Kent, J.Z. Sun, Ferromagnetic resonance study of polycrystalline cobalt ultrathin films, J. Appl. Phys. 99 (2006) 08N503, https://doi.org/10.1063/1.2151832.
[30] R. Urban, B. Heinrich, G. Woltersdorf, K. Ajdari, K. Myrtle, J.F. Cochran, E. Rozenberg, Nanosecond magnetic relaxation processes in ultrathin metallic films prepared by MBE, Phys. Rev. B 65 (2001) 020402(R), https://doi.org/10.1103/PhysRevB.65.020402.
[31] K.h. Zakeri, J. Lindner, I. Barsukov, R. Meckenstock, M. Farle, U. von Hörsten, H. Wende, W. Keune, J. Rocker, S. Kalarickal, K. Lenz, W. Kuch, K. Baberschke, Z. Frait, Spin dynamics in ferromagnets: Gilbert damping and two-magnon scattering, Phys. Rev. B 76 (2007), 104416, https://doi.org/10.1103/PhysRevB.76.104416.
[32] M.A.W. Schoen, D. Thonig, M.L. Schneider, T.J. Silva, H.T. Nembach, O. Eriksson, K.O.J.M. Shaw, Ultra-low magnetic damping of a metallic ferromagnet, Nat. Phys. 12 (2016) 839, https://doi.org/10.1038/nphys3770.
[33] Z. Xu, K. Zhang, J. Li, Disentangling intrinsic and extrinsic Gilbert damping, Phys. Rev. B 104 (22) (2021).
[34] J.C. Read, P.M. Braganca, N. Robertson, J.R. Childress, Magnetic degradation of thin film multilayers during ion milling, APL Mater. 2 (4) (2014) 046109, https://doi.org/10.1063/1.4870802.
[35] Z. Sun, S.T. Retterer, D. Li, The influence of ion-milling damage to magnetic properties of $Co_{80}Pt_{20}$ patterned perpendicular media, J. Phys. D: Appl. Phys. 47 (10) (2014) 105001, https://doi.org/10.1088/0022-3727/47/10/105001.
[36] R. Arias, D.L. Mills, Extrinsic contributions to the ferromagnetic resonance response of ultrathin films, Phys. Rev. B 60 (1999) 7395–7409, https://doi.org/10.1103/PhysRevB.60.7395.
[37] A.J. Lee, J.T. Brangham, Y. Cheng, S.P. White, W.T. Ruane, B.D. Esser, D.W. McComb, P.C. Hammel, F.Y. Yang, Metallic ferromagnetic films with magnetic damping under 1.4×10^{-3}, Nat. Commun. 8 (2017) 234, https://doi.org/10.1038/s41467-017-00332-x.